Electrical and optical properties of defects in silicon introduced by high-temperature electron irradiation

Jian-Guo Xu, Fang Lu, and Heng-Hui Sun
Physics Department, Fudan University, Shanghai, China
(Received 9 February 1988)

2-MeV electron irradiation of Si at elevated temperature creates a dominant deep level at the energy $E_c - 0.36$ eV in addition to the oxygen vacancies. This level, which is less significant in room-temperature-irradiated Si, is found to be an efficient recombination center in the present situation. The optical cross section of this level measured by deep-level optical spectroscopy reveals a fine structure superimposed on the main transition. This fine structure is considered to be related to a new resonant phonon mode coupled with the above defect. The isochronal annealing behavior shows that this defect might be a kind of vacancy-oxygen complex. With the assumption of a V_2-O_2 complex structure, a calculation based on the Green's-function method of lattice dynamics indicates the existence of a defect-induced resonant phonon mode with energy of 10 meV, which is in good agreement with the experimental observation.

I. INTRODUCTION

The effect of electron irradiation on silicon is an interesting topic in semiconductor physics because of its close relation with semiconductor-device technology. Defects in Si produced by high-energy electron irradiation have been used effectively as lifetime limiters in the fabrication of high-voltage rectifiers and thyristors, instead of gold diffusion, which would introduce some undesired thermal effects. Usually, the defects studied in previous works were produced by room-temperature electron irradiation.[1-3] Recently, electron irradiation under elevated temperature has been employed in semiconductor technology. The thermal stability of devices treated by high-temperature irradiation has proved to be better than those irradiated at room temperature. However, detailed studies on the physical properties of defects in high-temperature electron-irradiated Si have not been presented yet.

In this work, we report an investigation of electrical and optical properties of defects in Si introduced by high-temperature electron irradiation by using deep-level transient spectroscopy (DLTS) and deep-level optical spectroscopy (DLOS).[4] A new resonant phonon mode coupled with the defect has been identified and the structural configuration of the defect is suggested.

II. EXPERIMENT

The samples (p^+-n-n^+ diodes) were fabricated from an argon float-zoned n-type Si single crystal with a resistivity of 70 Ω cm. The electron irradiation was performed with a 2-MeV electron beam at a dose of 1×10^{14} electrons/cm^2 within the temperature range of 240–360 °C. As a comparison, another set of samples irradiated at room temperature was also investigated.

An EG&G 5206 lock-in amplifier was used as the rate window in the DLTS measurement. The lifetime of the minority carriers was determined by the reverse-recovery technique.[5] The DLOS method was used to measure the spectral distribution of the optical cross section of the deep level at temperatures of 60 and 80 K. In order to reduce the influence on the DLOS signals of electron capture and emission by the oxygen vacancies, the samples were subjected to thermal annealing at 350 °C for 175 min prior to the optical measurements.

III. RESULTS

A. Electrical properties

Figure 1 shows the DLTS of samples irradiated at 20 and 330 °C. The peaks E_2 and E_4 in the room-temperature-irradiated sample have been assigned as di-vacancies,[6] which are shown to be absent in the high-temperature-irradiated sample. Also shown in the latter

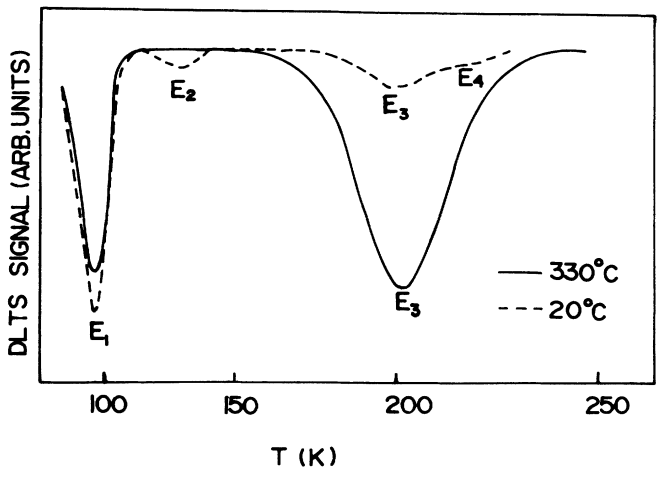

FIG. 1. DLTS of electron-irradiated samples. Solid curve, high-temperature (330 °C) irradiation; dashed curve, room-temperature (20 °C) irradiation. Lock-in frequency: 100 Hz.

case are the slight reduction of the concentration of E_1, which is believed to be related to the oxygen vacancy,[6] and an unknown level E_3 which is now the major peak in the spectrum. The energy level and electron thermal-capture cross section of E_3 are determined as $E_c - E_3 = 0.36$ eV and $\sigma_n^T = 1.0 \times 10^{-15}$ cm^2, respectively, where E_c is the conduction-band edge. The concentration of E_3 in the room-temperature-irradiated sample is so small, i.e., about one order of magnitude less than that of E_1, that little attention has been paid to this level in previous studies.

The introduction rates of levels E_1, E_2, and E_3 defined as the ratios of concentration N_T to irradiation dose Φ are found to vary with the irradiation temperature as shown in Fig. 2. Level E_2 disappears at a temperature of 270 °C, which is slightly lower than the temperature required to anneal out E_2 in the room-temperature-irradiated sample.[6] The concentration of E_3 reaches a maximum at 330 °C and exceeds that of E_1 beyond this temperature. Also shown in Fig. 2 is the temperature dependence of the minority-carrier lifetime τ. It can be seen that an increase of the concentration of E_3 corresponds to a decrease of τ and vice versa, while no such correlation between τ and the concentration of E_1 is observed. Therefore, it is reasonable to presume that E_3 is the major recombination center in the high-temperature-irradiated Si.

After the samples are thermally annealed within the temperature range of 20–300 °C, the lifetime changes as shown in Fig. 3 for the samples irradiated at 20 and 300 °C. The lifetime of the 300 °C-irradiated sample does not show a fluctuation like the room-temperature-irradiated one. This behavior improves the thermal stability of devices. In order to understand the cause of the lifetime variation, we measured the 20-min isochronal annealing properties of levels E_1, E_2, and E_3. The results are shown in Fig. 4. For the room-temperature-irradiated sample, a significant increase of E_3 accompanied by the reduction of E_1 and E_2 is observed beyond the temperature of 300 °C. This suggests that E_3 might

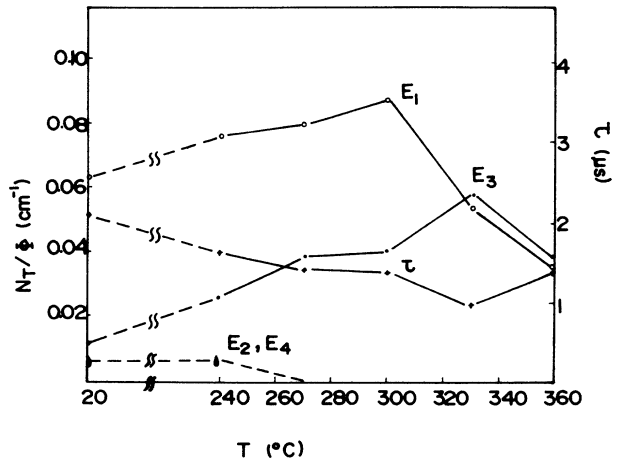

FIG. 2. Introduction rates of defects and minority-carrier lifetime vs irradiation temperature.

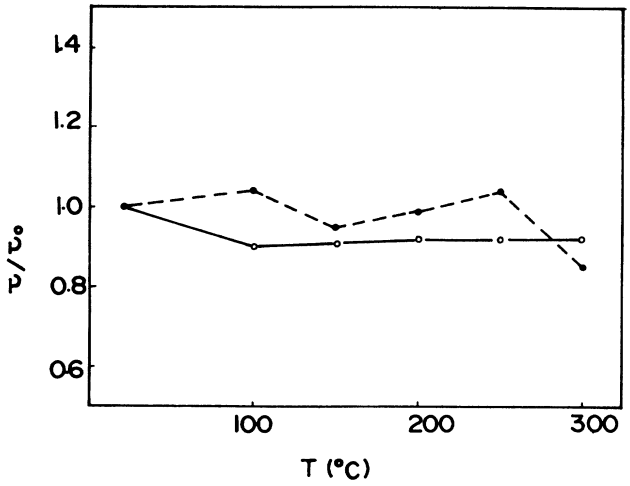

FIG. 3. Variation of minority carrier lifetime as a function of annealing temperature. Solid curve, 300 °C-irradiated sample; dashed curve, room-temperature-irradiated sample.

be a sort of vacancy-oxygen complex, which results from the decomposition and reassembly of divacancies and oxygen vacancies. The lifetime of minority carriers in the room-temperature-irradiated sample is controlled by both the divacancies E_2 and the level E_3 (Ref. 1). The concentration changes of these two levels are believed to be related to the instability of the lifetime with respect to the

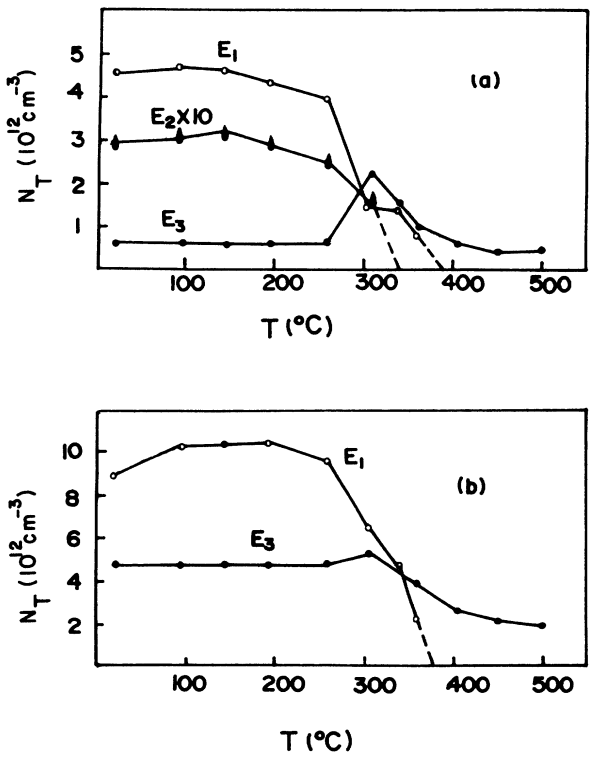

FIG. 4. 20-min isochronal annealing properties of the electron-irradiation-introduced defects. (a) Room-temperature-irradiated sample. (b) 300 °C-irradiated sample.

annealing temperature. For the high-temperature-irradiated sample, the concentration of E_3 is almost unchanged with annealing temperature until 300 °C, when a slight increase of E_3 is accompanied by a great reduction of E_1. All the multivacancies are almost annealed out in this sample;[3] hence it can be expected that the concentration of E_3 will not increase very much after isochronal annealing.

After thermal annealing, the concentration of E_3 could exceed greatly that of E_1 as shown in Fig. 4(b). We found that a 350 °C, 175-min thermal annealing of a 330 °C-irradiated sample could increase the concentration ratio of E_3 to E_1 up to a value of 12.8. In this case, electron capture and emission by level E_1 are negligible. It is quite favorable to use such a treatment in investigation of the optical properties of level E_3 by DLOS.

B. Optical properties

Figure 5 shows the measured optical-cross-section spectra $\sigma_n^o(h\nu)$ at 60 and 80 K. The major peak around $h\nu=0.38$ eV is believed to correspond to the optical transition from the E_3 level to the conduction band. A very interesting feature of the spectra is the existence of several equidistant (10 meV) small peaks superposed on the main peak. According to the following analysis, we attribute this fine structure to a phonon mode coupled with optical transitions via level E_3. No report concerning this phonon mode has been presented in previous DLOS works, although it is a quite well-known phenomenon in ir absorption and photoluminesce spectra of defects.

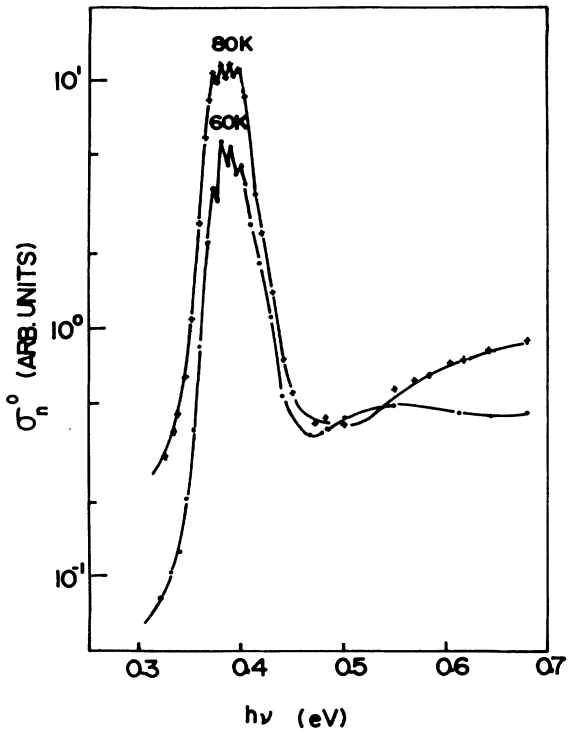

FIG. 5. DLOS of a 330 °C-irradiated sample treated by 350 °C, 175-min thermal annealing.

If the electron-phonon interaction is considered and the optical transition is treated by the adiabatic and Condon approximations, an expression of the optical cross section for the single-phonon-mode coupling could be derived as[7]

$$\sigma_n^o(h\nu)=\sum_{n,m=0}^{\infty}\{\sigma_{\rm el}^o[h\nu-E_3-(m-n)\hbar\omega] \times P_q(n,m,T)\}\ , \tag{1}$$

where

$$P_q(n,m,T)=(1-e^{-\hbar\omega/kT})e^{-n\hbar\omega/kT} \times e^{-\lambda}\left[\frac{n!}{m!}\right]\lambda^{m-n}[L_n^{m-n}(\lambda)]^2\ , \tag{2}$$

$$\sigma_{\rm el}^o \propto \frac{\frac{1}{h\nu}[h\nu-E_3-(m-n)\hbar\omega]^{\eta+1/2}}{\left[1+[h\nu-E_3-(m-n)\hbar\omega]\Big/\frac{\hbar^2a^2}{2m^*}\right]^{2\beta}}\ , \tag{3}$$

$\hbar\omega$ is the phonon-mode energy, λ the electron-phonon coupling strength, a^{-1} the bound-state wave-function extent, and $L_n^{m-n}(\lambda)$ the associated Laguerre polynomial. The parameter η has the value of zero (for a permitted transition) or unity (for a forbidden transition), and the value of β can be either 1 (for a δ-type potential) or 2 (for a Coulomb potential). If we assume that $\beta=2$ and $\eta=1$ and choose the following parameters: $\hbar\omega=10$ meV, $E_3=E_c-0.366$ eV, $\lambda=1.4$, and $a^{-1}=20$ Å, the calculated optical-cross-section spectrum at 60 K coincides fairly well with the observation, as shown in Fig. 6. The phonon energy $\hbar\omega$ and energy position of E_3 are the same as the experimental values from DLOS and DLTS results. The assumption of a Coulomb potential ($\beta=2$) agrees with the fact that the thermal-capture cross section σ_n^T of E_3 decreases monotonically with the temperature.[8] The forbidden transition indicates that the bound-state wave

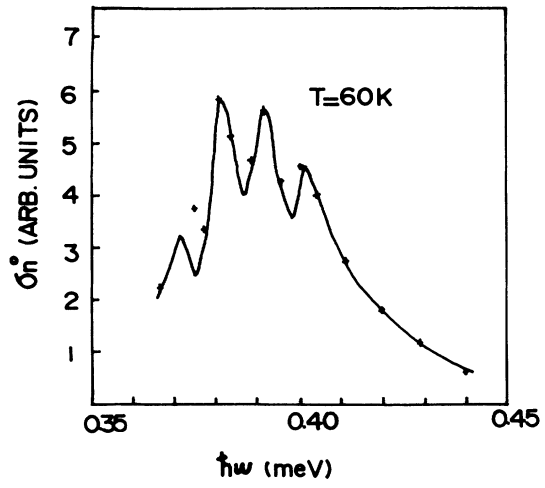

FIG. 6. The coincidence of calculated optical-cross-section fine structure (solid curve) with experimental data (+) based upon a phonon-defect interaction hypothesis.

function of level E_3 possesses s-like symmetry.[7] The Franck-Condon shift of E_3 thus can be derived as $d_{FC}=\lambda\hbar\omega=14$ meV.

IV. DISCUSSION

It can be seen from the phonon spectrum of a perfect Si lattice that the phonon density of states almost vanishes at the energy of 10 meV (80 cm^{-1}).[9] Hence, the 10-meV phonon mode in DLOS might be an extrinsic mode induced by the E_3 defect. It is likely a kind of resonant phonon mode with the vibrational wave function localized at the vicinity of the defect.[10] Since the phonon mode is closely related to the nature and the structural configuration of the defect, it can be theoretically treated by the Green's-function method of lattice dynamics. The generalized lattice-dynamical equation is

$$M_{\alpha\mu(l)}\frac{d^2U_{\alpha\mu}(l,t)}{dt^2}+\sum_{l',\alpha',\mu'}\phi_{\alpha\mu\alpha'\mu'}U_{\alpha'\mu'}(l',t)=0 \tag{4}$$

where $M_{\alpha\mu}(l)$ is the mass of the atom, $\phi_{\alpha\mu\alpha'\mu'}$ the force-constant matrix element, and $U_{\alpha\mu}(l,t)$ the displacement along the α direction of the μth atom in the l unit cell at time t. The matrix expression of Eq. (4) is

$$\hat{M}\frac{d^2\mathbf{u}}{dt^2}+\hat{\phi}\mathbf{u}=0\ . \tag{5}$$

If the Green's-function matrix of a nonperfect lattice is defined as

$$\hat{G}=(\hat{M}\omega^2-\hat{\phi})^{-1} \tag{6}$$

and the perturbation matrix is

$$\hat{C}=(\hat{M}^0-\hat{M})\omega^2+\hat{\phi}^0-\hat{\phi}\ , \tag{7}$$

then

$$\hat{G}=(\hat{g}\hat{C}-1)^{-1}\hat{g} \tag{8}$$

where

$$\hat{g}=(\hat{M}^0\omega^2-\hat{\phi}^0)^{-1} \tag{9}$$

is the Green's-function matrix of a perfect Si lattice, and $\hat{M}^0$ and $\hat{\phi}^0$ are the matrices corresponding to the perfect lattice. The phonon density of states can be expressed as[11]

$$\mathcal{D}(\omega)=-\frac{2\omega}{3rN}\lim_{\varepsilon\to 0}\mathrm{Im}\mathrm{Tr}[\hat{M}^{1/2}\hat{G}(\omega+i\varepsilon)\hat{M}^{1/2}] \tag{10}$$

where r is the number of atoms per unit cell and N the number of unit cells in the crystal. From the definition of (7), we know that $\hat{C}$ remains nonzero only at a very small region near the defect; therefore the calculation of $\hat{G}$ is also restricted to this limited region. It has been pointed out in the preceding section that E_3 is believed to be a kind of vacancy-oxygen complex. Here, we assume it is a V_2-O_2 complex.[12] From considerations of symmetry and stability, the configuration of E_3 is possibly composed of two V-O defects occurring at two substitutional sites neighboring each other as shown in the inset of Fig. 7. The problem then could be simplified to a calculation of the vibration mode of a V-O defect pair. The $\hat{G}$ matrix could be further reduced due to the C_{3v} symmetrical properties of the V-O pair. Since both the atomic mass and force constant would be changed as the Si atoms are substituted by V-O defects, the following parameters were used in the calculation: (1) the change of force constant along the interconnections of two V-O pairs, i.e., $\delta_\parallel=\hat{\phi}^0_\parallel-\hat{\phi}_\parallel$; (2) the change of force constant perpendicular to the interconnections of V-O, i.e., $\delta_\perp=\hat{\phi}^0_\perp-\hat{\phi}_\perp$; and (3) the relative change of atomic mass $(M_{Si}-M_{V\text{-}O})/M_{Si}$, which is a constant, 3/7. Only $\delta_\parallel$ and $\delta_\perp$ are adjustable parameters. The values of the Green's function $\hat{g}$ for a perfect Si lattice was taken from Elliott and Pfeuty.[9] Figure 7 shows the calculated phonon spectrum, where $\delta_\parallel$ and $\delta_\perp$ were chosen to be 1×10^4 and 2×10^4 dyn/cm^2, respectively. The phonon density of states here shows a strong peak at 10 meV. This gives substantial support to our suggestion that the assignment of E_3 to a V_2-O_2 defect is conceptually preferable.

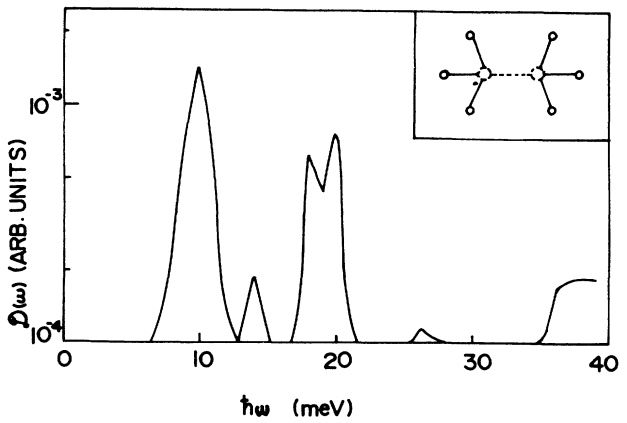

FIG. 7. Calculated phonon spectrum of Si when there exist V_2-O_2 defects. The inset is the assumed configuration of E_3.

In conclusion, we observed a deep-level energy $E_c-0.36$ eV in the high-temperature electron-irradiated Si which is verified to be an efficient recombination center. The isochronal annealing experiments associated with the DLOS measurements show that it might be a defect with the structural configuration of V_2-O_2 that induced a 10-meV new phonon mode revealed in the measured optical-cross-section spectra.

ACKNOWLEDGMENTS

The assistance in sample preparation by M. Zeng-Guang Zhang and Liang Wang at Shanghai Rectifier Factory is greatly appreciated. This work was supported by the National Natural Science Foundation of China.

[1]A. O. Evwaraye and B. J. Baliga, J. Electrochem. Soc. **124**, 913 (1977).

[2]S. D. Brotherton and P. Bradley, J. Appl. Phys. **53**, 5720 (1982).

[3]J. W. Corbett, in *International Conference on Radiation Effects in Semiconductors, Dubrovnik, 1976,* Inst. Phys. Conf. Ser. No. 31, edited by N. B. Urli and J. W. Corbett (IOP, Bristol, 1977), p. 8.

[4]A. Chantre, G. Vincent, and D. Bois, Phys. Rev. B **23**, 5335 (1981).

[5]D. C. Lewis, Solid State Electron. **18**, 87 (1975).

[6]L. C. Kimerling, in *International Conference on Radiation Effects in Semiconductors, Dubrovnik, 1976,* Inst. Phys. Conf. Ser. No. 31, edited by N. B. Urli and J. W. Corbett (IOP, Bristol, 1977), p. 221.

[7]B. Monemar and L. Samuelson, Phys. Rev. B **18**, 809 (1978).

[8]Rong-Ping Den (private communication).

[9]R. J. Elliott and P. Pfeuty, J. Phys. Chem. Solids **28**, 1789 (1967).

[10]P. G. Dawber and R. J. Elliott, Proc. R. Soc. London, Ser. A **273**, 222 (1963).

[11]Harald Bottger, *Principle of the Theory of Lattice Dynamics* (Akademie-Verlag, Berlin, 1983), p. 88.

[12]Y. H. Lee and J. W. Corbett, Phys. Rev. B **13**, 2653 (1976).